UDC 546.05, 546.02

DOI: 10.15372/CSD2020202

Mechanochemical Synthesis of Carbonate- and Fluoride-Substituted Hydroxyapatite

S. V. MAKAROVA[1], N. V. BULINA[1,2], M. V. CHAIKINA[1], I. YU. PROSANOV[1], V. R. KHUSNUTDINOV[1]

[1]*Institute of Solid State Chemistry and Mechanochemistry, Siberian Branch, Russian Academy of Sciences, Novosibirsk, Russia*

[2]*Novosibirsk State University, Novosibirsk, Russia*

E-mail: sveta070796@mail.ru

Abstract

Hydroxyapatite, fluoroapatite, and hydroxyapatite with partial substitution by fluoride and carbonate ions were obtained through mechanochemical synthesis. When a fluoride ion is introduced into the structure of hydroxyapatite, the substitution of the hydroxyl group occurs, while carbonate ion substitutes the phosphate group. Lattice parameters and the CSR of the samples were refined using the Rietveld method. It was found that the introduction of substituents into the structure of hydroxyapatite reduces the lattice parameters, which is due to the smaller size of substituting ions. The synthesized powders can be used in medicine as bioresorbable materials.

Keywords: mechanochemical synthesis, hydroxyapatite, carbonate apatite, fluoroapatite, fluoride-substituted hydroxyapatite

INTRODUCTION

Hydroxyapatite (HA) is the major component of bone and dental tissues. Synthetic HA is a biocompatible, osteoconstructive and biodegradable material that is ideally suitable for bone tissue regeneration [1–3]. Due to these properties, HA is also interesting as a material for bone implants [4, 5]. Hydroxyapatite is widely used in the form of granules and ceramic products to fill bone defects in craniofacial surgery, when high mechanical strength is not necessary [6, 7]. The technology of 3D printing opens broad possibilities for the application of HA in the manufacture of bioresorbable implants with complicated structure and required shapes [8].

The properties of materials used to manufacture implants are affected by the presence of substituting ions in the structure of apatite. Substitutions for fluoride and carbonate anions in HA structure are among the most important ones. It is known that fluoroapatite is more chemically stable than HA, especially in the acid medium. Due to this property, fluoroapatite is widely used in stomatological preparations to protect enamel [9]. Carbonate apatite possesses high biocompatibility with the mineral component of human bones; its presence enhances the rate of HA bioresorption [10].

Various methods of HA synthesis are known, such as precipitation, sol-gel procedure, ceramic and mechanochemical methods [11]. Mechanochemical synthesis (MCS) is a rather simple method to obtain nano-sized HA without the use of solvents, so there is no need to carry out additional stages to purify the product [12, 13]. During MCS, chemical reactions are stimulated by the energy released in the impacts and friction of balls rotating continuously at a high speed. Energy release depends on the technical characteristics of the mill [14, 15].

The goal of the work was to synthesize fluoride- and carbonate-substituted HA by means of MCS using a planetary ball mill.

EXPERIMENTAL

The synthesis of fluoride- and carbonate-substituted HA was carried out using the mechanochemical method in an AGO-2 planetary mill (Russia) with steel vials. The volume of each vial was 150 ml, the mass of milling bodies 0.8 cm in diameter was 200 g, the rate of vial rotation among the axis was 1800 r.p.m. To avoid iron abrasion in the products, the vials were lined with a mixture of initial reagents before synthesis. MCS was carried out for 30 min.

Initial reagents were anhydrous calcium hydroorthophosphate $CaHPO_4$ (Ch. – pure reagent grade), annealing calcium oxide CaO (Ch. reagent grade) and calcium fluoride CaF_2 (Ch. D. A. – pure for analysis reagent grade). Initial reagents were introduced in the stoichiometric ratios according to equations

$$4CaO + 6CaHPO_4 \rightarrow Ca_{10}(PO_4)_6(OH)_2 + 2H_2O \quad (1)$$

$$3.95CaO + 6CaHPO_4 + 0.05CaF_2 \rightarrow Ca_{10}(PO_4)_6F_{0.1}(OH)_{1.9} + 3H_2O \quad (2)$$

$$3CaO + 6CaHPO_4 + CaF_2 \rightarrow Ca_{10}(PO_4)_6F_2 + 3H_2O \quad (3)$$

$$4CaO + 5CaHPO_4 + CO_2\ (air) \rightarrow Ca_9(PO_4)_5(CO_3)(OH) + 2H_2O \quad (4)$$

$$3CaO + 6CaHPO_4 + CO_2\ (air) \rightarrow Ca_9(HPO_4)(PO_4)_5(OH) \cdot 2H_2O + CO_2\ (air) \quad (5)$$

Here (1) is the reaction describing the formation of non-substituted HA; (2) is the partial substitution of OH-groups by F^- ions, (3) is the complete substitution of OH-groups by F^- ions (4) is the substitution of phosphate ions by carbonate ions; (5) is Ca-deficient HA with the substitution of phosphate ions by hydrophosphate ions.

To achieve a higher crystallinity degree, the synthesized samples were annealed at a temperature of 1100 °C for 2 h in a PVK 1.4-8 electric furnace (Russia) with the rate of temperature rise 5 °C/min.

XRD patterns were recorded with the help of a powder diffractometer D8 Advance (Bruker, Germany) in Bragg-Brentano geometry with CuK_α radiation. X-ray phase analysis of the compounds was carried out using the database of powder diffraction patterns ICDD PDF-4 (2011). Refinement of unit cell parameters, the size of the region of coherent scattering – coherent length (CSR) and the concentrations of phases were calculated using the Rietveld method in Topas 4.2 software (Bruker, Germany). FTIR spectra were recorded with the help of an Infralyum-801 spectrometer (Russia) using the procedure of sample pelleting by pressing with KBr powder. Carbonate content was determined using the manometric method.

RESULTS AND DISCUSSION

Fluoroapatite and fluorohydroxyapatite

The diffraction patterns of the samples after MCS are shown in Fig. 1, *a*. One can see that all samples are identical, and reflections correspond to HA phase (card PDF [040-10-6315]). The

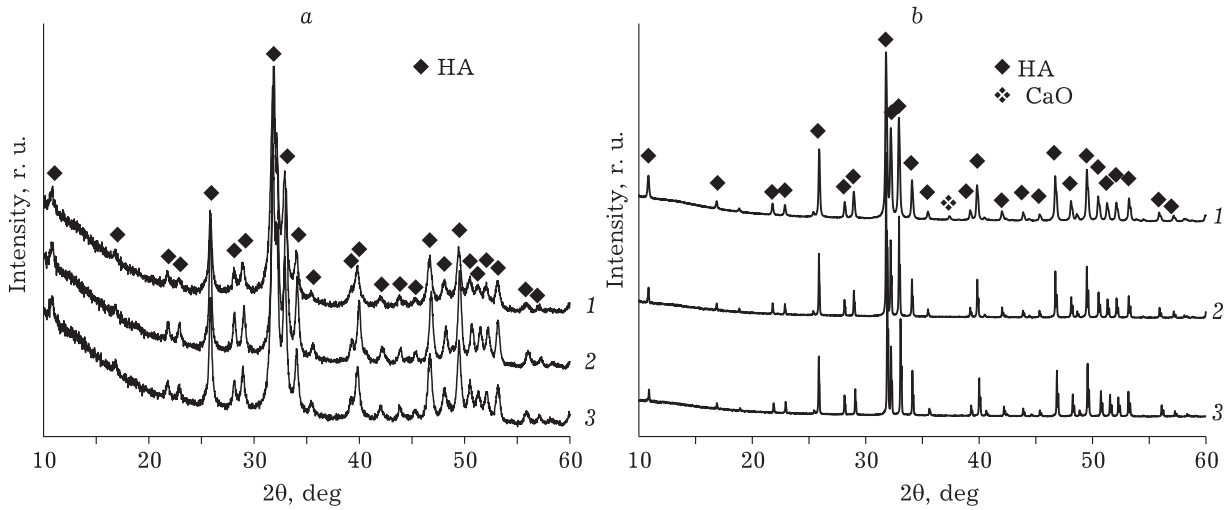

Fig. 1. XRD patterns of samples obtained according to reactions (1)–(3): after MCS (*a*) and after annealing at 1100 °C (*b*). Here and in Fig. 2–4: spectra are numbered in agreement with the numbers of reactions according to which the samples were synthesized.

TABLE 1

Structural characteristics of synthesized samples

Reaction No.	Cell parameter, Å		Unit cell volume, Å^3	CSR, nm
	a	*c*		
1	9.433(4)	6.895(3)	531.3(5)	20.6(8)
2	9.427(6)	6.892(5)	530.4(8)	32.0(7)
3	9.388(3)	6.890(2)	525.9(4)	26.0(7)
4	9.426(2)	6.896(3)	530.6(4)	22.6(2)
5	9.430(2)	6.889(2)	532.8(2)	21.5(2)

diffraction patterns of fluorosubstituted HA after annealing also reveal only one phase, while the diffraction patterns of unsubstituted HA contains an admixture phase (4 mass %) of calcium oxide (see Fig. 1, *b*).

Refinement of lattice parameters with the help of the Rietveld method showed that the parameter *a* decreases with an increase in the concentration of fluoride ion introduced (Table 1). Parameter *c* decreases insignificantly. These changes lead to *a* decrease in the unit cell volume and are explained by the fact that the radius of fluoride ion (1.33 Å) is smaller than the radius of the substituted OH-ion (1.53 Å), which is located on *c* axis of the hexagonal lattice of HA [16]. Similar changes were observed also by other authors for fluoroapatite synthesized by means of deposition [17]. So, a decrease in the value of parameter *a* points to the fact that F^- substitutes OH^-. The average size of crystallites in the sample varies within the nanometer range: 20–32 nm.

The FTIR spectra (Fig. 2, *a*) of the mechanochemically synthesized samples under investigation, obtained according to reactions (1)–(3), contain the major bands of the absorption of phosphate group in HA (570, 601, 964, 1048, 1091 cm^{-1}), and their positions are identical in all samples. The positions of the absorption bands of hydroxyl group (627, 3573 cm^{-1}) depend on the concentrations of the introduced fluoride ion. The absorption band of the stretching vibrations of OH-group in the FTIR spectrum of the sample obtained according to reaction (2) shifts to lower frequencies (3552 cm^{-1}). This band is not detected in the sample obtained according to reaction (3), in which hydroxyl groups are absent. The libration vibration of OH-group shifts after the introduction of F^- to higher frequencies (688 cm^{-1}), and the second absorption band appears (745 cm^{-1}). These changes were observed also by other authors [17]. A shift of the absorption bands of OH-groups is explained by the effect of fluoride ion localized in the nearest surroundings of the hydroxyl group. FTIR spectra also contain weak absorption bands of carbonate ion (870, 1400–1500 cm^{-1}) incorporated into HA structure during synthesis.

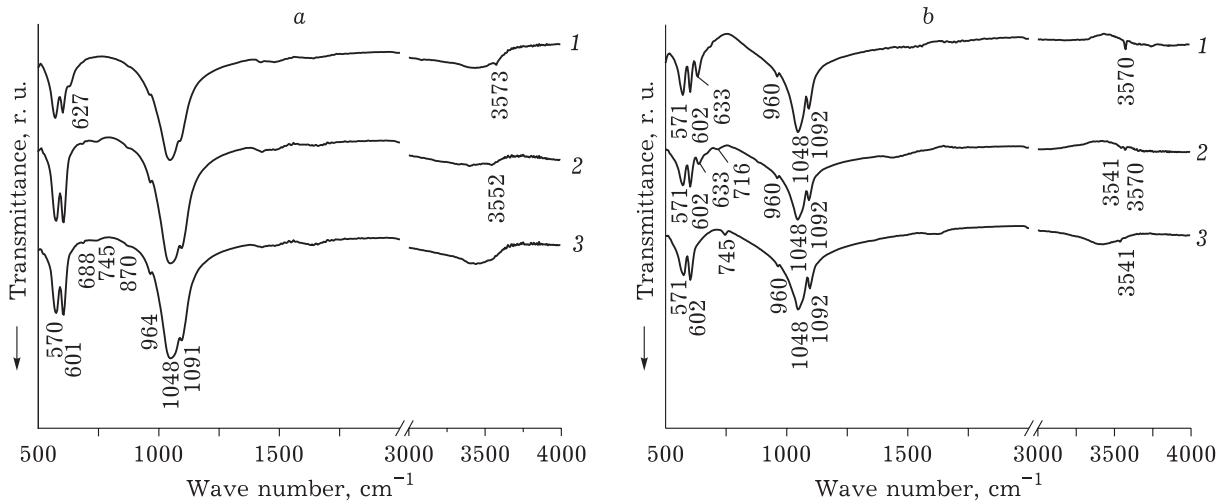

Fig. 2. FTIR spectra of the samples obtained according to reactions (1)–(3): after MCS (*a*) and after additional annealing at 1100 °C (*b*). For designations, see Fig. 1.

The FTIR spectra of annealed samples (see Fig. 2, *b*) reveal the disappearance of the absorption bands of carbonate ion and a more clear manifestation of the weak bands corresponding to the absorption of hydroxyl group. The FTIR spectrum of the sample obtained according to reaction (2) contains two bands of libration vibrations of OH-group (633, 716 cm^{-1}) and two bands of stretching vibrations (3541 and 3570 cm^{-1}). Relying on literature data [18], we may suppose that the sample contains two types of OH-groups: 1) located at a position which is remote from the fluoride ion (characterized by bands at 3570 and 633 cm^{-1}); 2) located at a position in the vicinity of fluoride ion (characterized by vibrations at the frequency of 3544 and 716 cm^{-1}). These vibrations point to the introduction of F^- into HA structure.

Carbonatehydroxyapatite

One can see in the material presented above that the synthesis of stoichiometric HA according to reaction (4) involves the capture of CO_2 molecules, which are built into the forming HA lattice and occupy the positions of phosphate ions in the form of CO_3^{2-}. Because of this, a question arises whether the MCS of HA containing no carbonate ions is possible. To answer this question, the synthesis according to reaction (5) was carried out.

One can see in the diffraction patterns shown in Fig. 3, a that the samples obtained according to reactions (4) and (5) are identical, reflections correspond to the only phase HA. It follows from Table 1 that *a* parameter for carbonate-substituted HA (4) is smaller than that for non-substituted one (1) and calcium-deficient HA (5). This is explained by the fact that the ion radius of CO_3^{2-} (1.81 Å) is smaller than that of PO_4^{3-} (2.12 Å) [16], which leads to a decrease in parameter *a* in the case when some phosphate groups are substituted by carbonate groups. The average size of crystallites of the synthesized apatite samples is in the nanometer range: 20–23 nm.

To confirm the formation of calcium-deficient HA according to reaction (5), the products of MCS were annealed at 1100 °C. Diffraction patterns (see Fig. 3) exhibit the reflections of beta-tricalcium phosphate phase (β-TCP), which is the product of decomposition of calcium-deficient HA according to reaction:

$$Ca_9(HPO_4)(PO_4)_5(OH) \xrightarrow{t} 3Ca_3(PO_4)_2 + H_2O \qquad (6)$$

Carbonatehydroxyapatite does not contain this phase, however, the reflections of CaO appeared. Thermal decomposition of carbonatehydroxyapatite proceeds according to the reaction:

$$6Ca_9(PO_4)_5(CO_3)(OH) + 2H_2O \xrightarrow{t} 4CaO + 5Ca_{10}(PO_4)_6(OH)_2 + 6CO_2\uparrow \qquad (7)$$

The FTIR spectra of the mechanochemically synthesized samples under investigation (Fig. 4, *a*) obtained according to reactions (4) and (5) contain the major bands of the absorption of phosphate groups in HA (570, 601, 964, 1048 and 1091 cm^{-1}) and the hydroxyl group of HA (627, 3573 cm^{-1}). The FTIR spectrum of the product of reaction (4) contains absorption bands of carbonate group (875, 1426, 1469, 1639 cm^{-1}), which confirms that CO_3^{2-} ion enters the position of phosphate ion [19]. The FTIR spectrum of the product of MCS

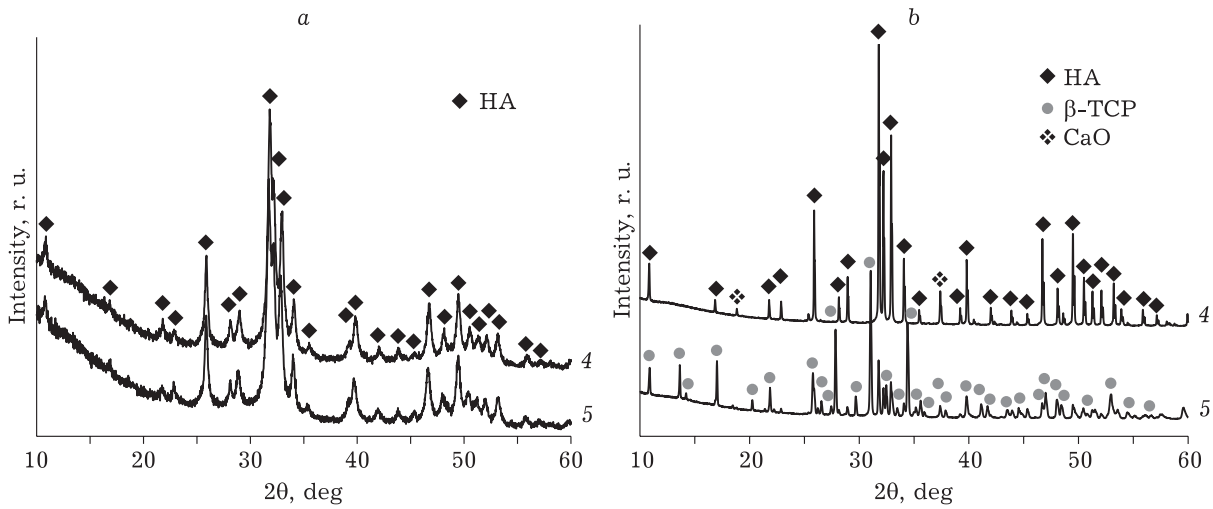

Fig. 3. XRD patterns of the samples obtained according to reactions (4) and (5): after MCS (*a*) and after additional annealing at 1100 °C (*b*). For designations, see Fig. 1.

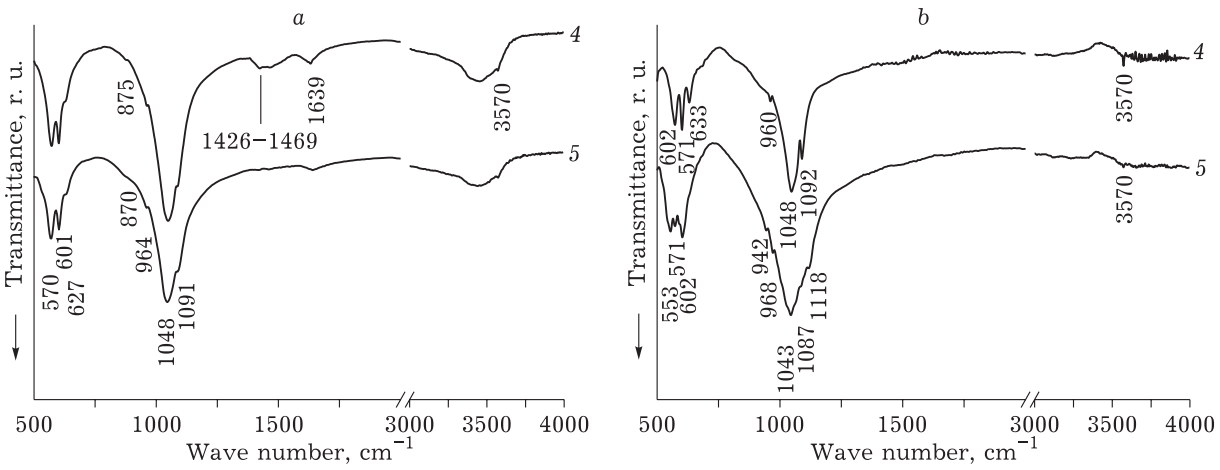

Fig. 4. FTIR spectra of the samples obtained according to reactions (4) and (5): after MCS (*a*) and after additional annealing at 1100 °C (*b*). For designations, see Fig. 1.

according to reaction (5) does not contain the bands related to carbonate ion, but there is a weak band of HPO_4^{2-} absorption (870 cm^{-1}) [20]. The data of manometric analysis confirm the absence of carbonate in the sample obtained according to reaction (5). The content of CO_3^{2-} ion in the sample synthesized according to reaction (4) was 1.39 mass %.

The FTIR spectra of annealed samples (see Fig. 4, *b*) do not contain the bands of carbonate group adsorption, which points to the fact that CO_3^{2-} comes out of HA structure. The spectrum of the sample obtained according to reaction (5) contains the absorption bands of orthophosphate group of β-TCP (553, 602, 942, 968, 1043 and 1118 cm^{-1}) [21], which agrees with the data of X-ray phase analysis described above.

CONCLUSION

Fluoroapatite, fluoride-substituted HA with substitution degree 0.1 mol per 1 mol of HA, carbonate-substituted HA with substitution degree 1 mol per 1 mol of HA, and calcium-deficient HA containing no carbonate ion were synthesized using the mechanochemical method by means of mechanical treatment for 30 min. It was established that the introduction of fluoride ions into HA structure causes a decrease in parameter *a*, while parameter *c* remains almost unchanged, which points to the substitution of hydroxide ion in HA structure by fluoride ion. The introduction of carbonate ion into the structure of apatite also causes a decrease in lattice parameter *a*. It is established that mechanochemical synthesis may be used to obtain nanometer-sized fluoride- and carbonate-substituted HA that may be then used in medicine to make bioresorbable 3D-products.

Acknowledgements

The investigation was carried out with the financial support from RFBR under project No. 18-29-11064.

REFERENCES

1 Farag M. M., Yun H.-S., Effect of gelatin addition on fabrication of magnesium phosphate-based scaffolds prepared by additive manufacturing system, *Mater. Letters*, 2014, Vol. 132, P. 111–115.

2 Rodriguez G., Dias J., d'Avila M. A., Bartolo P., Influence of hydroxyapatite on extruded 3D scaffolds, *Procedia Engin.*, 2013, Vol. 59, P. 263–269.

3 Ang T. H., Sultana F. S. A., Hutmacher D. W., Wong Y. S., Fuh J. Y. H., Mo X. M., Teoh S. H., Fabrication of 3D chitosan-hydroxyapatite scaffolds using a robotic dispensing system, *Mater. Science and Engin.: C*, 2002, Vol. 20, No. 1–2, P. 35–42.

4 Lee J. S., Seol Y. J., Sung M., Moon W., Kim S. W., Oh J. H., Cho D. W., Development and analysis of three-dimensional (3D) printed biomimetic ceramic, *Inter. J. Precision Engin. and Manuf.*, 2016, Vol. 17, No. 12, P. 1711–1719.

5 Li X., Zhang S., Zhang X., Xie S., Zhao G., Zhang L., Biocompatibility and physicochemical characteristics of poly (Ɛ-caprolactone)/poly (lactide-co-glycolide)/ nano-hydroxyapatite composite scaffolds for bone tissue engineering, *Mater. and Design*, 2017, Vol. 114, P. 149–160.

6 Cortez P. P., Atayde L. M., Silva M. A., Armada-da-Silva P., Fernandes M. H., Afonso A., Santos J. D., Characterization and preliminary in vivo evaluation of a novel modified hydroxyapatite produced by extrusion and spheronization techniques, *J. Biomed. Mater. Res. Part B: Appl. Biomat.*,

2011, Vol. 99, No. 1, P. 170–179.
7 Staffa G., Nataloni A., Compagnone C., Servadei F., Custom made cranioplasty prostheses in porous hydroxy-apatite using 3D design techniques: 7 years experience in 25 patients, *Acta Neurochirurgica*, 2007, Vol. 149, No. 2, P. 161–170.
8 Tian X., Günster J., Melcher J., Li D., Heinrich J. G., Process parameters analysis of direct laser sintering and post treatment of porcelain components using Taguchi's method, *J. Europ. Cer. Soc.*, 2009, Vol. 29, No. 10, P. 1903–1915.
9 De Leeuw N. H., Density functional theory calculations of local ordering of hydroxy groups and fluoride ions in hydroxyapatite, *Physic. Chem. Chem. Phys.*, 2002, Vol. 4, No. 15, P. 3865–3871.
10 Lu X., Zhao Z., Leng Y., Calcium phosphate crystal growth under controlled atmosphere in electrochemical deposition, *J. Crystal Growth*, 2005, Vol. 284, No. 3–4, P. 506–516.
11 Sadat-Shojai M., Synthesis methods for nanosized hydroxyapatite with diverse structures, *Acta Biomaterialia*, 2013, Vol. 9, No. 8, P. 7591–7621.
12 Silva C. C., Graзa M. P. F., Valente M. A., Sombra A. S. B., Crystallite size study of nanocrystalline hydroxyapatite and ceramic system with titanium oxide obtained by dry ball milling, *J. Mater. Science*, 2007, Vol. 42, No. 11, P. 3851–3855.
13 Fahami A., Ebrahimi-Kahrizsangi R., Nasiri-Tabrizi B., Mechanochemical synthesis of hydroxyapatite/titanium nanocomposite, *Solid State Sciences*, 2011, Vol. 13, No. 1, P. 135–141.
14 Mochales C., Wilson R. M., Dowker S. E., Ginebra M. P., Dry mechanosynthesis of nanocrystalline calcium deficient hydroxyapatite: Structural characterisation, *J. Alloys and Compounds*, 2011, Vol. 509, No. 27, P. 7389–7394.
15 Silva C. C., Pinheiro A. G., De Oliveira R. S., Goes J. C., Aranha N., De Oliveira L. R., Sombra A. S. B., Properties and in vivo investigation of nanocrystalline hydroxyapatite obtained by mechanical alloying, *Mater. Science and Engin.: C*, 2004, Vol. 24, No. 4, P. 549–554.
16 Lurie Yu. Yu., Handbook of Analytical Chemistry, M.: Khimiya, 1989. 448 c.
17 Wei M., Evans J. H., Bostrom T., Grшndahl L., Synthesis and characterization of hydroxyapatite, fluoride-substituted hydroxyapatite and fluorapatite, *J. Mater. Science: Mater. in Med.*, 2003, Vol. 14, No. 4, P. 311–320.
18 Nikcevic I., Jokanovic V., Mitric M., Nedic Z., Makovec D., Uskokovic D., Mechanochemical synthesis of nanostructured fluorapatite/fluorhydroxyapatite and carbonated fluorapatite/fluorhydroxyapatite, *J. Solid State Chem.*, 2004, Vol. 177, No. 7, P. 2565–2574.
19 Rehman I., Bonfield W., Characterization of hydroxyapatite and carbonated apatite by photo acoustic FTIR spectroscopy, *J. Mater. Science: Mater. in Med.*, 1997, Vol. 8, No. 1, P. 1–4.
20 Pazourková L., Hundáková M., Peikertová P., Martynková G. S., Preparation of calcium-deficient hydroxyapatite particles on vermiculite by precipitation and sonication, *J. Australian Cer. Society*, 2017, Vol. 53, No. 2, P. 775–785.
21 Lin J. C., Kuo K. H., Ding S. J., Ju C. P., Surface reaction of stoichiometric and calcium-deficient hydroxyapatite in simulated body fluid, *J. Mater. Science: Mater. in Med.*, 2001, Vol. 12, No. 8, P. 731–741.